Nonlinear Three-Port Magnetic-Circuit Element for Ferromagnetic Yokes of Accelerator Magnets

Herbert De Gersem[1], Vaishnavi Srinivasan[1,2], and Carsten Muehle[2]
[1]Institut für Theorie Elektromagnetischer Felder (TEMF), TU Darmstadt, Germany, degersem@temf.tu-darmstadt.de
[2]Helmholtzzentrum für Schwerionenforschung GSI, Darmstadt, Germany

A rectangular ferromagnetic yoke part where a part of the magnetic flux is branched off sidewards to an air region can be modeled by a nonlinear three-port magnetic equivalent circuit. The model incorporates a 1D FE model which accounts for the complicated interplay of saturation and fringing. The method is applied to a combined-function accelerator magnet.

***Index Terms*—Accelerator magnets, Finite element analysis, Newton method, Nonlinear network analysis.**

I. Introduction

MAGNETIC equivalent circuits (MECs) are a popular modeling tool for simulating electrical devices [1] and provide a remarkable accuracy when the magnetic flux paths can be predicted effectively [2]. Even in the presence of ferromagnetic parts, a nonlinear MEC is a very efficient design tool [3], [4], [5]. In situations with complicated field patterns, accurate equivalent MEC parameters can be extracted from finite-element (FE) models, as long as the flux can be assumed to be homogeneous at the ports [6]. However, a problem arises when saturation and fringing effects interfere with each other. In this paper, a nonlinear three-port MEC is constructed for a magnetic path where a part of the flux branches-off at its side and enters an air region.

II. Linear Three-Port MEC Element

Consider the bottom leg of the magnet yoke of Fig. 1 around which a coil with N turns and a current I is wound. For a straight flux path (model A), the standard model is the combination of a magnetic voltage source $\Theta = NI$ and a reluctance $\mathcal{R}_{\mathrm{yk,hor}} = \frac{a}{\mu \ell_z b}$ with μ the permeability, a the path length and $\ell_z b$ the path's cross-section (method A).

For the situation in model B, the above approach is not applicable. Nevertheless, the magnetic field problem can be solved analytically. Derived from that, one finds a relation between the magnetic voltage drops Θ_1 and Θ_2 and the fluxes Φ_1 and Φ_2 (method B), i.e.,

$$\begin{bmatrix} \Theta_1 \\ \Theta_2 \end{bmatrix} = \begin{bmatrix} \frac{NI}{2} \\ \frac{NI}{2} \end{bmatrix} + \begin{bmatrix} \mathcal{R}_\ell + \mathcal{R}_\mathrm{t} & \mathcal{R}_\mathrm{t} \\ \mathcal{R}_\mathrm{t} & \mathcal{R}_\ell + \mathcal{R}_\mathrm{t} \end{bmatrix} \begin{bmatrix} \Phi_1 \\ \Phi_2 \end{bmatrix} . \tag{1}$$

where the values for the reluctances are $\mathcal{R}_\ell = \frac{a}{2\mu\ell_z b}$ and $\mathcal{R}_\mathrm{t} = \frac{3b}{8\mu\ell_z a}$. Eq. (1) corresponds to the equivalent scheme shown in Fig. 1 (method B) and can be embedded as such in a standard MEC solver.

III. Straightforward Nonlinear Three-Port MEC Element

When ferromagnetic saturation becomes important, a nonlinear MEC is set up. Straightforward nonlinear counterparts of the above linear MEC elements are constructed by updating the reluctance according to the operating point on the BH-characteristic evaluated for the magnetic field strength found by dividing the magnetic voltage by the magnetic path length. For the elements $\mathcal{R}_\ell$ and $\mathcal{R}_\mathrm{t}$, the path lengths are identified to be $\frac{a}{2}$ and $\frac{3b}{8}$, respectively. The equations are linearized by the Newton method. This simple procedure, however, neglects the fact that saturation may change the pattern of the magnetic flux distribution. Saturation may locally invoke a reluctivity which becomes comparable with the reluctivity of air. Then, a change of the flux pattern is expected, especially when a part of the flux branches off towards an air region.

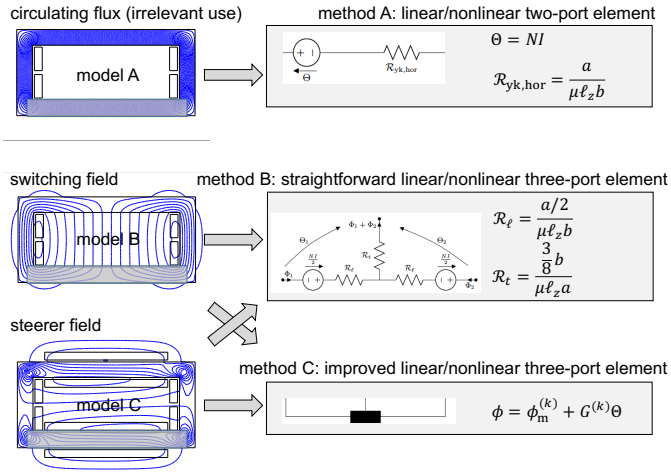

Fig. 1. Overview of the applied methods and exemplary models: Model A shows a technically irrelevant operating mode of the magnet where the flux circulates around the yoke; Model B provides a switching field, whereas model C provides a steerer field. Each method presents a circuit equivalent for a single yoke leg: Method A gives a (non)linear two-port element; Method B provides a (non)linear three-port element; Method C provides an improved nonlinear three-port element.

IV. Improved Nonlinear Three-Port MEC Element

An improved nonlinear three-port MEC element is set up for the exemplary bottom leg of Model C (Fig. 1). For a short

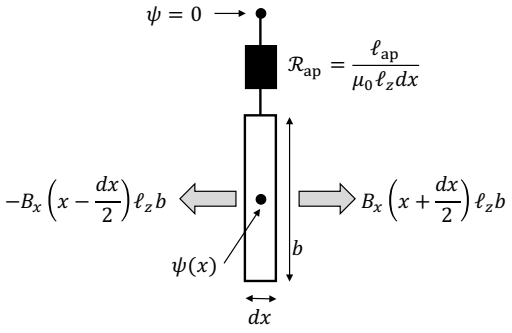

Fig. 2. Elementary piece for determining a 1D model including saturation and fringing.

slice (see Fig. 2), flux conservation is expressed by

$$-B_x\left(x-\frac{dx}{2}\right)b\ell_z + B_x\left(x+\frac{dx}{2}\right)b\ell_z + \frac{\mu_0 \ell_z dx}{\ell_{\mathrm{ap}}/2}\psi(x) = 0 \quad , \tag{2}$$

where $B_x(x)$ is the x-component of the magnetic flux density, dx is the slice thickness, $b\ell_z$ is the yoke cross-section and ℓ_{ap} is the vertical aperture length. By introducing the nonlinear material characteristic $B = \mu(|H|)B$ and the relation $H_x(x) = -\frac{\mathrm{d}\psi}{\mathrm{d}x}$, one finds the 1D differential equation

$$-\frac{\mathrm{d}}{\mathrm{d}x}\left(\mu\left(|H(x)|\right)\frac{\mathrm{d}\psi(x)}{\mathrm{d}x}\right) + \frac{2\mu_0}{\ell_{\mathrm{ap}} b}\psi(x) = 0 \quad . \tag{3}$$

Eq. (3) is linearized by Newton's method and discretized along the magnetic path by 1D piecewise hat functions. After convergence of the nonlinear iteration, a relation between the magnetic voltages Θ_{port} and the fluxes Φ_{port} at the ports is extracted, yielding an expression of the form

$$\Phi_{\mathrm{port}} = \mathcal{G}_{\mathrm{port}}\Theta_{\mathrm{port}} + \Phi_{\mathrm{m,port}} \quad , \tag{4}$$

with $\mathcal{G}_{\mathrm{port}}$ a permeance matrix and $\Phi_{\mathrm{m,port}}$ a source-permeance vector. This model can be represented by the circuit of Fig. 3 and treated as such in a standard MEC solver. The overall simulation procedure consists of a nonlinear MEC simulation (outer iteration) where in each iteration a nonlinear 1D FE problem is solved (inner iteration).

V. Example and Conclusions

A combined-function magnet is developed as part of a new injection line for the FAIR project at the Helmholtzzentrum für Schwerionenforschung GSI [7]. The magnet can generate a vertical magnetic field for bending the particle beam in the horizontal plane, thereby switching between one or another beam line. Additionally, the magnet can generate a horizontal magnetic field to adjust the beam in the vertical plane. When operated in a nonlinear regime, however, both functions may interfere [8], [9]. The simulation results obtained by linear and nonlinear MEC models are compared to those from a FE model serving as a reference in Fig. 4. In linear operation, the MEC and FE simulation results match almost perfectly. In saturation, however, the straightforward nonlinear MEC is inaccurate. The approach with the improved nonlinear three-port MEC element has a better accuracy but still can not compete with FE simulation for high saturation levels.

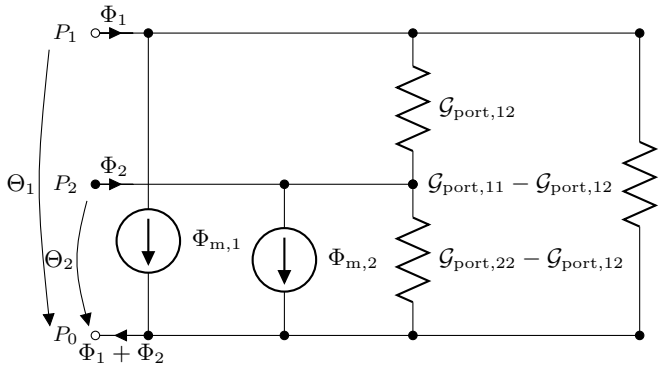

Fig. 3. Nonlinear three-port element.

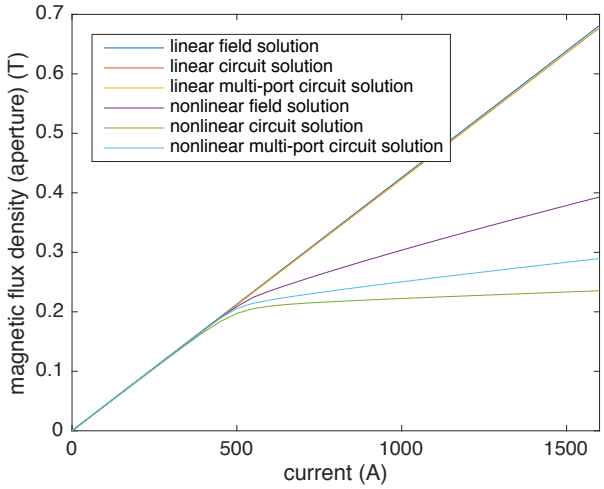

Fig. 4. Magnetic flux density in the aperture of the bending magnet.

References

[1] M. Amrhein and P. T. Krein, "3-D magnetic equivalent circuit framework for modeling electromechanical devices," *IEEE Trans. Energ. Convers.*, vol. 24, no. 2, pp. 397–405, jun 2009.

[2] A. Demenko and J. Sykulski, "Network equivalents of nodal and edge elements in electromagnetics," *IEEE Trans. Magn.*, vol. 38, no. 2, pp. 1305–1308, 2002.

[3] M. Moallem and G. Dawson, "An improved magnetic equivalent circuit method for predicting the characteristics of highly saturated electromagnetic devices," *IEEE Trans. Magn.*, vol. 34, no. 5, pp. 3632–3635, sept 1998.

[4] H. W. Derbas, J. M. Williams, A. C. Koenig, and S. D. Pekarek, "A comparison of nodal- and mesh-based magnetic equivalent circuit models," *IEEE Trans. Energ. Convers.*, vol. 24, no. 2, pp. 388–396, jun 2009.

[5] S. D. Sudhoff, B. T. Kuhn, K. A. Corzine, and B. T. Branecky, "Magnetic equivalent circuit modeling of induction motors," *IEEE Trans. Energ. Convers.*, vol. 22, no. 2, pp. 259–270, jun 2007.

[6] V. Ostović, "A simplified approach to magnetic equivalent-circuit modeling of induction machines," *IEEE Trans. Ind. Appl.*, vol. 24, no. 2, pp. 308–316, mar/apr 1988.

[7] GSI. (2016) Helmholtzzentrum für Schwerionenforschung GSI. [Online]. Available: www.gsi.de

[8] J. Tanabe, "Iron dominated electromagnets design, fabrication, assembly and measurements," Stanford Linear Accelerator Center, Stanford Synchrotron Radiation Laboratory, Tech. Rep. SLAC-R-754, Jan. 2005.

[9] T. Zickler, "Basic design and engineering of normal-conducting, iron-dominated electromagnets," CERN Accelerator School, 2009.